Chinese Chemical Letters 33 (2022) 2625–2629

Contents lists available at ScienceDirect

Chinese Chemical Letters

journal homepage: www.elsevier.com/locate/cclet

Preparation of a porphyrin-polyoxometalate hybrid and its photocatalytic degradation performance for mustard gas simulant 2-chloroethyl ethyl sulfide

Ying Yang[a], Fangsheng Tao[a], Lijuan Zhang[a,*], Yunshan Zhou[a,*], Yuxu Zhong[b,*], Shubo Tian[a], Yong'an Wang[b]

[a] State Key Laboratory of Chemical Resource Engineering, Institute of Chemistry, Beijing University of Chemical Technology, Beijing, 100029 China
[b] Toxicology and Medical Countermeasures, Beijing Institute of Pharmacology and Toxicology, Beijing, 100850, China

ARTICLE INFO

Article history:
Received 1 September 2021
Revised 22 September 2021
Accepted 25 September 2021
Available online 30 September 2021

Keywords:
Chemical warfare agent
Mustard gas simulant
Porphyrin
Polyoxometalate
Photooxidation

ABSTRACT

By combining 5,10,15,20-tetra(4-chlorine)phenylporphyrin (TClPP) and α-Keggin polyoxometalate $H_5PV_2Mo_{10}O_{40}$ (H_5PVMo) *via* a simple ion-exchange method, an organic-inorganic hybrid material $[C_{44}H_{28}N_4Cl_4]_{1.5}[H_2PMo_{10}V_2O_{40}]\cdot 2C_2H_6O$ (H_2TClPP-H_2PVMo) was prepared and thoroughly characterized by a variety of techniques. The homogeneous photocatalytic degradation of 2-chloroethyl ethyl sulfide (CEES) (5 μL) by H_2TClPP-H_2PVMo (1×10^{-6} mol/L) was studied in methanol and methanol-water mixed solvent (v/v = 1:1), in which the degradation rate of CEES reached 99.52% and 99.14%, respectively. The reaction followed first-order reaction kinetics, and the half-life and kinetic constant in methanol and the mixed solvent were respectively 33.0 min, −0.021 min^{-1} and 15.7 min, −0.043 min^{-1}. Mechanism analysis indicated that under visible light irradiation in the air, CEES was degraded *via* oxidation and alcoholysis/hydrolysis in methanol and the mixed solvent. $O_2^{\cdot-}$ and $^1O_2$ generated by H_2TClPP-H_2PVMo selectively oxidized CEES into a nontoxic sulfoxide. Singlet oxygen capture experiments showed that H_2TClPP-H_2PVMo (ϕ = 0.73) had a higher quantum yield of singlet oxygen than TClPP (ϕ = 0.35) under an air atmosphere and visible light irradiation.

Mustard gas (HD) is an erosive agent that can cause blisters on human skin, irritate the eyes and respiratory tract, and even cause death and other hazards; thus, much research has been conducted to find methods to protect against HD [1–4]. The degradation pathway of HD mainly includes hydrolysis [5], dehydrohalogenation [6,7] and oxidation [8]. Among them, the degradation of HD through hydrolysis and dehydrohalogenation generally occurs slowly and incompletely [6,9]. In recent years, the research on the degradation of HD has mainly focused on oxidative degradation. Under oxidizing conditions, HD may be over-oxidized to produce toxic bis(2-chloroethyl)sulfone (HDO_2) or be selectively oxidized to nontoxic bis(2-chloroethyl)sulfoxide (HDO) [10,11]; thus, it is important to find a suitable catalyst to selectively oxidize it to the sulfoxide form. Singlet oxygen can selectively oxidatively degrade HD, as well as its analog, CEES, into HDO and CEESO rather than over-oxidize them to HDO_2 and $CEESO_2$, respectively [12,13]. This provides a method for the green degradation of HD.

As a common organic photosensitizer, porphyrin can generate singlet oxygen. Halogen atoms have a heavy-atom effect, so porphyrin molecules with halogen atoms have a stronger ability to generate singlet oxygen [14,15]. They have been widely used in research fields such as photodynamic therapy [16,17] and photocatalysis [18,19]. The disadvantage is that porphyrins tend to self-aggregate in solvents, which reduces their ability to generate singlet oxygen [20,21]. To solve this problem, a few metal-organic frameworks (MOFs) with porphyrin as the organic linker have been synthesized (in which porphyrin moieties are isolated by the porous, three dimensional nature of the framework, that is beneficial to generate singlet oxygen) and shown good degradation effects for the photocatalytic degradation of CEES [22,23]. These results encourage further exploration for optimization of the photosensitizers in other type of systems for HD decontamination. polyoxometalates are a class of metal-oxygen cluster compounds formed by transition metal ions (high valence states of V, Mo, W, *etc.*) through the coordination and bridging of oxygen atoms [24–

* Corresponding authors.
E-mail addresses: ljzhang@mail.buct.edu.cn (L. Zhang), zhouys@mail.buct.edu.cn (Y. Zhou), yuxuzhong2008@aliyun.com (Y. Zhong).

https://doi.org/10.1016/j.cclet.2021.09.093
1001-8417/

30]. They have a suitable oxidizing ability [31–33] and have been used to catalytically oxidize and degrade HD and CEES. Among them, α-Keggin-type $H_5PV_2Mo_{10}O_{40}$ (H_5PVMo) has been used as an oxidizing active material, and air (O_2) or H_2O_2 has been used as an oxidant to selectively oxidize the erosive agent HD and its simulant CEES to their sulfoxide forms [34,35]. In recent years, porphyrin polyoxometalate organic-inorganic hybrid materials have attracted attention due to the unique characteristics of porphyrins and polyoxometalates. Under acidic conditions, the N atom in the middle of the porphyrin ring can be protonated to form a divalent porphyrin cation [36]. The proton-containing polyoxometalate is strongly acidic. When the polyoxometalate containing a proton encounters a porphyrin, it can donate a proton to transform the porphyrin into a divalent cation. Then, it becomes a polyoxometalate anion that finally combines cationic porphyrin through electrostatic interactions to form an ionic porphyrin-polyoxometalate hybrid [37,38]. Although porphyrin-polyoxometalate hybrid materials have not been reported for the degradation of HD, the photocatalytic reactions in which they are involved with good repeated use performance has been well documented [39,40], for example, photocatalytic oxidation of alcohols [39], and degradation of rhodamine and other organic pollutants [40]. Thus, it is worth exploring their application for the photocatalytic oxidation of HD and CEES.

Based on the above analysis, this paper selected photosensitive 5,10,15,20-tetra(4-chlorine)phenylporphyrin (TClPP) with four halogen atoms and the Keggin-type polyoxometalate H_5PVMo metal cluster to synthesize a new organic-inorganic hybrid material $[C_{44}H_{28}N_4C_{l4}]_{1.5}[H_2PMo_{10}V_2O_{40}]\cdot 2C_2H_6O$ (H_2TClPP-H_2PVMo). This material has a higher singlet oxygen generation capacity than TClPP in the air under visible light irradiation. It uses generated singlet oxygen $^1O_2$ and superoxide radical $O_2^{\cdot-}$ to selectively oxidize CEES to nontoxic CEESO (Supporting information). As a homogeneous catalyst, H_2TClPP-H_2PVMo has excellent repeated use performance for the degradation of CEES and has potential application value in chemical war agent defense and degradation.

Fig. S2 (Supporting information) shows the infrared spectra of TClPP, H_5PVMo, and H_2TClPP-H_2PVMo, in which the band positions of TClPP and H_5PVMo are consistent with those reported in the literature [41,42]. In the infrared spectrum of H_2TClPP-H_2PVMo, the characteristic bands of P-O_a of H_5PVMo move to the direction of low wave number, and the characteristic bands of Mo-O_b-Mo and Mo-O_c-Mo move to the direction of high wave number. This indicates the presence of interactions between the anion and cation that lead to formation of the H_2TClPP-H_2PVMo hybrid. Fig. S3 (Supporting information) shows the ^1H NMR spectrum of TClPP and the ^{31}P solid-state NMR spectrum of H_2TClPP-H_2PVMo, further verifying the successful synthesis of the H_2TClPP-H_2PVMo hybrid material (for detailed infrared and nuclear magnetic spectra, see Supporting information).

To understand the interactions between TClPP and H_5PVMo in solution, spectrometric titration experiment was carried out. Fig. 1 shows changes in the ultraviolet spectra during the addition of ethanol H_5PVMo solution to dichloromethane TClPP solution. When the solution contained only TClPP, two obvious absorption bands of porphyrin appeared in the ultraviolet spectrum: a strong S band at 418 nm and medium-intensity Q band at 514, 549, 588 and 645 nm [43]. When the ethanol H_5PVMo solution was gradually added to the dichloromethane TClPP solution, the absorption bands of the ultraviolet spectrum at 415, 514 and 549 nm gradually decreased, and new absorption peaks appeared at 454 and 682 nm. As the amount of H_5PVMo increased, the intensity of the peaks also increased. The UV spectrum at this time was not equal to the sum of the UV spectrum of the two individual materials, indicating that TClPP and H_5PVMo have strong interactions during the dropping process. The inset in Fig. 1 (*viz*., part b) has a low-intensity

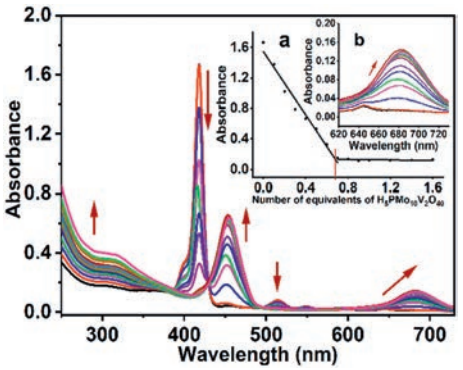

Fig. 1. The spectrum evolution of H_5PVMo titration of TClPP. Inset: (a) The linear fit of the absorbance at 415 nm to the molar ratio of C_{H_5PVMo}/C_{TClPP}; (b) Magnified spectra from 620 nm to 730 nm. The direction of the arrow represents an increase or decrease in the absorption with the addition of H_5PVMo.

absorption band at 647 nm. This means that during the dropping of H_5PVMo, TClPP first accepted a proton to form a monoprotonated salt, and continued to accept protons until it became a deprotonated salt [36,44]. The inset in Fig. 1 (part a) shows that when the H_5PVMo in the solution was less than 0.67 times the amount of TClPP (the stoichiometric ratio was less than 1:1.5), the addition of H_5PVMo had a linear decolorizing effect on the S band of TClPP. When the stoichiometric ratio of H_5PVMo to TClPP reached 1:1.5, the S band of TClPP has an obvious turning point, indicating that TClPP and H_5PVMo formed a stable Table 1.5:1 organic-inorganic hybrid [45,46]. This is in good agreement with the elemental analysis results (Supportin information).

As shown in Fig. S4 (Supportin information), the TG-DTA curve of H_2TClPP-H_2PVMo includes three weight loss processes. In general, the thermogravimetric analysis and elemental analysis were consistent.

In this paper, the photocatalytic degradation of CEES by H_2TClPP-H_2PVMo in methanol was first studied. As shown in Fig. 2, upon extending the reaction time, the degradation rate of CEES by H_2TClPP-H_2PVMo increased gradually. When the reaction time was 180 min, the degradation rate of CEES reached 99.52%, and continuing to extend the reaction time caused the degradation rate to increase very slowly.

To further understand the material's ability to catalytically oxidatively degrade CEES, determine the active components in methanol and necessity of the participation of light in the reaction, this paper compares the degradation performance of H_2TClPP-H_2PVMo, TClPP, and H_5PVMo on CEES with/without light. As shown in Fig. 3, when the reaction time was 180 min, H_5PVMo had a degradation rate of about 20% for CEES with/without light. This is because H_5PVMo can catalyze and oxidize CEES in the presence of oxygen/air [34,35], which is unaffected by the light conditions. The degradation rate of H_2TClPP-H_2PVMo to CEES under irradiation was 99.52%, while the degradation rate without illumination was only 28.24%. This shows that light significantly promoted the decontamination of CEES by H_2TClPP-H_2PVMo. The degradation rate of TClPP to CEES with/without irradiation was 55.31% and 5.23%, respectively. It can be seen that the sum of degradation rate of H_5PVMo (20%) and TClPP (55.31%) to CEES was lower than that of the H_2TClPP-H_2PVMo hybrid (99.52%). The degradation rate of CEES in the blank group without any components with/without irradiation was about 4.2%, further indicating necessity of the participation of light in the reaction.

HD and its analog CEES can be hydrolyzed in water, but their lipophilicity gives them low solubility in water. The rate of hydrolysis was limited by controlling the mass transfer rate. Adding organic solvents to water can increase the amount of CEES in the

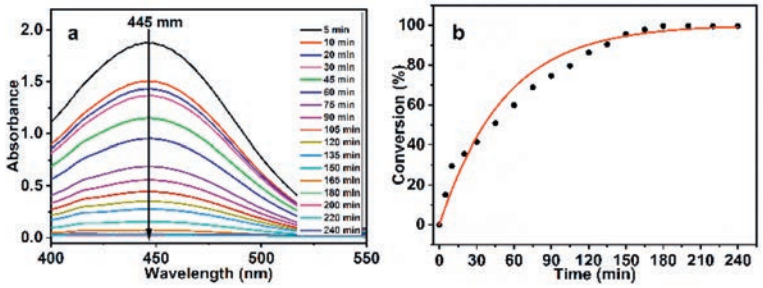

Fig. 2. UV absorbance spectra of the degradation of CEES by H_2TClPP-H_2PVMo (a) at different reaction times and (b) corresponding degradation rate. Degradation conditions: 500 W xenon lamp (λ > 400 nm); reaction solvent volume and catalyst concentration: 5 μL CEES in 5 mL methanol, $c = 1 \times 10^{-6}$ mol/L.

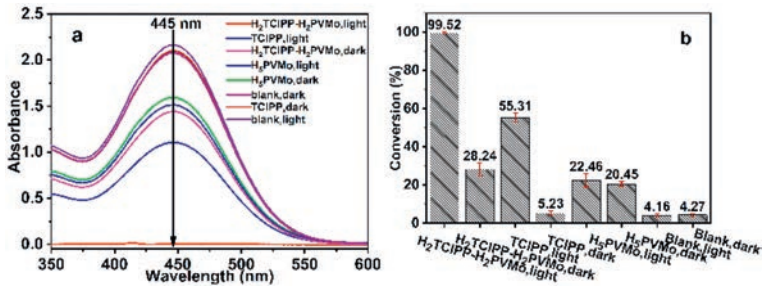

Fig. 3. (a) UV–vis absorbance spectra and (b) comparison of the degradation performance of CEES by H_2TClPP-H_2PVMo, TClPP and H_5PVMo in methanol. Degradation conditions: 500 W xenon lamp (λ > 400 nm), 5 μL CEES in 5 mL methanol, H_2TClPP-H_2PVMo (1×10^{-6} mol/L), TClPP (1.5×10^{-6} mol/L), H_5PVMo (1×10^{-6} mol/L), reaction time 180 min.

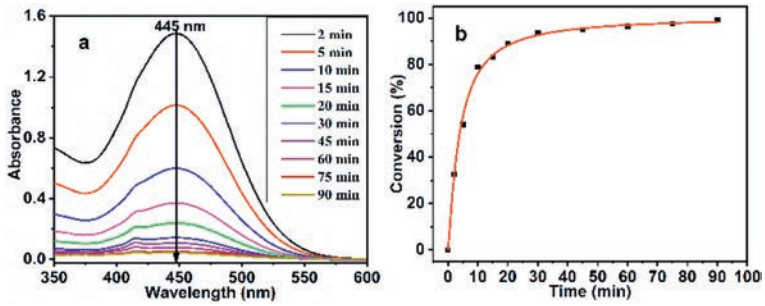

Fig. 4. (a) The UV–vis absorbance spectra and (b) degradation rate of CEES by H_2TClPP-H_2PVMo in mixed solvents. Reaction conditions: 500 W xenon lamp (λ > 400 nm); reaction solvent volume and catalyst concentration: 5 μL CEES in 5 mL methanol-water mixed solvent (v:v = 1:1), $c = 1 \times 10^{-6}$ mol/L.

solvent, and its increased solubility increased the rate of hydrolysis [47,48]. Therefore, this article continues to explore the degradation of H_2TClPP-H_2PVMo in a mixed solvent of methanol and water (1:1, v/v), and other reaction conditions remained unchanged. The results are shown in Fig. 4. It can be seen that as the reaction time increased, the degradation rate of H_2TClPP-H_2PVMo in the mixed solvent gradually increased. When the reaction time was 90 min, the degradation rate of CEES reached 99.14%.

To further understand the catalytic oxidative degradation of CEES in the mixed solvent and the need for light during the reaction, the degradation performance of H_2TClPP-H_2PVMo, TClPP, and H_5PVMo on CEES with/without light was compared. The results are shown in Fig. 5. When the reaction time was 90 min, the degradation rate of H_2TClPP-H_2PVMo to CEES without light was 91.05%, which is basically equal to the blank group, while H_2TClPP-H_2PVMo degraded more CEES under irradiation with the degradation rate 99.14% of CEES.

Then, the kinetics of the catalytic degradation of CEES by H_2TClPP-H_2PVMo in methanol and methanol-water solvents were studied. As shown in Fig. S5 (Supporting information), the relationship between ln (C_{CEES}) and reaction time is shown. By fitting the graph of ln (C_{CEES}) to reaction time, the kinetic curve of the degradation of CEES by H_2TClPP-H_2PVMo was obtained. The results showed a linear relationship. When using methanol or methanol-water mixed solvent, the reaction process conformed to first-order reaction kinetics. From the kinetics curve, it can be seen that the degradation half-life and reaction rate constant of H_2TClPP-H_2PVMo in methanol and methanol-water solvents were 33.0 min, −0.021 min^{-1} and 15.7 min, −0.043 min^{-1}, respectively.

In this paper, the repeated usage of H_2TClPP-H_2PVMo during the photocatalytic degradation of CEES in methanol-water solvent was studied. Each time CEES was added, the reaction was 90 min, and it was added five times in a row. As shown in Fig. S6 (Supporting information), the degradation rate after the fifth addition is 98.1%, indicating that H_2TClPP-H_2PVMo can be repeatedly used to degrade CEES.

To further study the photocatalytic degradation mechanism of CEES by H_2TClPP-H_2PVMo in methanol, GC–MS was used to analyze the degradation products of CEES (Fig. 6 and Fig. S7 in Supporting information). As shown in Fig. 6, under irradiation in the air, CEES generated 2-methoxyethyl ethyl sulfide by alcoholysis in methanol [49]. A small amount of ethyl 2-hydroxyethyl sulfide (HEES) was hydrolyzed due to the presence of a small amount of water in the solvent [47,48]. When the catalyst H_2TClPP-H_2PVMo

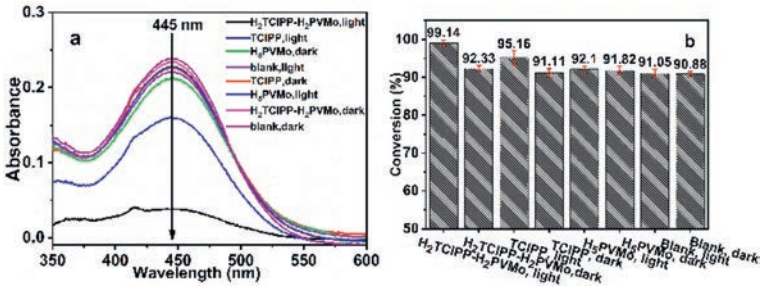

Fig. 5. (a) UV–vis absorbance spectra and (b) comparison of the degradation performance of CEES by H_2TClPP-H_2PVMo, TClPP and H_5PVMo in mixed methanol-water solvents. Degradation conditions: 500 W xenon lamp ($\lambda > 400$ nm); reaction solvent volume: 5 μL CEES in 5 mL methanol-water mixed solvent (v:v = 1:1); H_2TClPP-H_2PVMo (1×10^{-6} mol/L), TClPP (1.5×10^{-6} mol/L), H_5PVMo (1×10^{-6} mol/L), 5 μL.

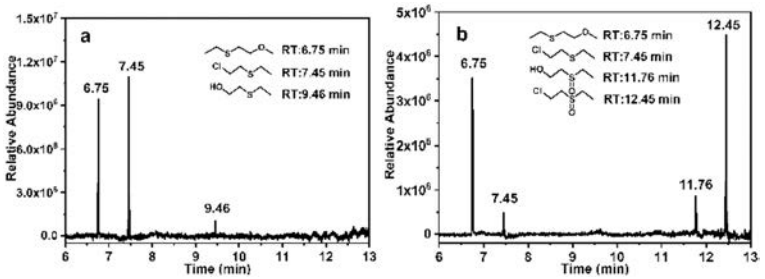

Fig. 6. GC chromatograms of the degradation products of CEES in the (a) absence and (b) presence of H_2TClPP-H_2PVMo in methanol. Reaction conditions: 500 W xenon lamp ($\lambda > 400$ nm), reaction time: 180 min, catalyst concentration: $c = 1 \times 10^{-6}$ mol/L.

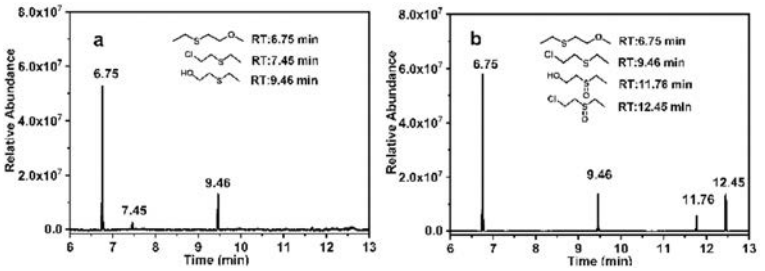

Fig. 7. GC chromatograms of the degradation products of CEES in the (a) absence and (b) presence of H_2TClPP-H_2PVMo in the methanol-water mixed solvent. Reaction conditions: 500 W xenon lamp ($\lambda > 400$ nm), reaction time: 90 min, catalyst concentration: $c = 1 \times 10^{-6}$ mol/L.

was added to methanol under irradiation, in addition to a small amount of unreacted CEES, two new oxidation products appeared: ethyl hydroxyethyl sulfoxide (HEESO) and 2-chloroethyl ethyl sulfoxide (CEESO). These may have appeared because, under irradiation, H_2TClPP-H_2PVMo is expected to produce active oxygen that selectively oxidized CEES and HEES to their sulfoxide forms [12,13,50–52]. This made up for the inadequacy of general oxidants to over-oxidize them into toxic meson sulfone.

The photocatalytic degradation mechanism of CEES and H_2TClPP-H_2PVMo in the methanol-water mixed solvent was also studied using GC–MS (Fig. 7 and Fig. S8 in Supporting information). As shown in Fig. 7, under irradiation in the air, the methanol-water mixed solvent permitted the alcoholysis [49] and hydrolysis [47,48] of CEES to generate 2-methoxyethane, ethyl sulfide, and ethyl 2-hydroxyethyl sulfide (HEES). H_2TClPP-H_2PVMo in the methanol-water mixed solvent photocatalytically degraded CEES products in addition to forming 2-methoxyethyl ethyl sulfide. Ethyl 2-hydroxyethyl sulfoxide (HEES) also produced two oxidation products, ethyl 2-hydroxyethyl sulfoxide (HEESO) and 2-chloroethyl ethyl sulfoxide (CEESO). The CEESO may have been generated due to the direct oxidation of CEES by active oxygen generated by H_2TClPP-H_2PVMo [53]. HEESO formed due to the degradation of CEES by the methanol-water mixed solvent and H_2TClPP-H_2PVMo, which may be the result of the mixed solvent. CEES was hydrolyzed to produce HEES [47,48], and then H_2TClPP-H_2PVMo generated active oxygen under irradiation and continued to oxidize HEES to HEESO [50–52].

To determine the reactive oxygen species produced in the degradation of CEES by H_2TClPP-H_2PVMo in methanol solvent and the $^1O_2$ production capacity of H_2TClPP-H_2PVMo, we carried out active oxygen identification and singlet oxygen capture experiments. According to the experimental results in Table S1, the degradation rate of CEES was 99.14% when no scavenger was added. After adding benzoquinone or NaN_3, the degradation rate of CEES decreased to 64.54% and 43.67%, respectively. The degradation rate of CEES decreased to 26.72% after adding both benzoquinone and NaN_3 at the same time, indicating that H_2TClPP-H_2PVMo degraded CEES by producing $O_2^{\cdot-}$ and $^1O_2$ in methanol with visible light irradiation. As shown in Fig. S9 (Supporting information), the $^1O_2$ quantum yield of TClPP in methanol was $\phi = 0.35$, and the $^1O_2$ quantum yield of H_2TClPP-H_2PVMo in methanol was $\phi = 0.73$, indicating that the ionic H_2TClPP-H_2PVMo hybrid formed by the interaction of H_2TClPP and H_2PVMo significantly increased the quantum yield of $^1O_2$ compared with TClPP. This effectively compensated for the self-aggregation of porphyrin in the solvent, which led to an insufficient quantum yield of $^1O_2$. We next explored the fluorescence emission spectra of H_2TClPP and H_2TClPP-H_2PVMo. As shown in Fig. S10 (Supporting informa-

tion), the fluorescence intensity of H_2TClPP-H_2PVMo was less than that of H_2TClPP. This may be because H_2TClPP-H_2PVMo has more energy to excite the singlet state under irradiation to reach the excited triplet state *via* energy transfer [15,54] to produce more singlet oxygen. This results in less energy being returned from the excited singlet state to the ground state, which is manifested as a decrease in the fluorescence intensity.

Table S2 (Supporting information) summarizes the photocatalytic degradation of CEES using different catalysts. Currently, most catalysts used to degrade CEES are metal-organic frameworks. Although the photocatalytic degradation rate of CEES is fast, most reaction conditions require pure O_2 and high-energy ultraviolet light, and the preparation of the catalysts with good yield still need to be explored. In contrast, the preparation method of the material synthesized in this paper is simple, and the generated $^1O_2$ and O_2 can be used to degrade CEES under an air atmosphere and visible light irradiation.

In summary, the as-prepared organic-inorganic hybrid material H_2TClPP-H_2PVMo exhibited excellent performance for the photocatalytic degradation of CEES in methanol and methanol-water mixed solvents. As a homogeneous catalyst, the material has good reusability and has great potential application value for the degradation of HD using natural or artificial light. We thought that presence of polyoxometalate may not only reduce the aggreciation of porphyrins in the solution but also interfere the mechanism of singlet oxygen generation in the hybrid system due to the ionic interaction between anionic polyoxometalate moieties and cationic prophyrin moieties. Careful theoretical investigation on the unrevealed reason accounting for the excellent performance in photocatalytic degradation of CEES of the hybrid material is still undertaken in our group. Considering the variety of polyoxometalates and porphyrins, it is expected that more efficient porphyrin-polyoxometalate hybrid catalysts will be designed and synthesized for the degradation of chemical war agents.

Declaration of competing interest

The authors declare that they have no known competing financial interests or personal relationships that could have appeared to influence the work reported in this paper.

Acknowledgments

The financial support from the Natural Science Foundation of China (No. 21976013) and kind support from Prof. Xue Duan of Beijing University of Chemical Technology is greatly acknowledged.

Supplementary materials

Supplementary material associated with this article can be found, in the online version, at doi:10.1016/j.cclet.2021.09.093.

References

[1] C.Y. Yu, J.A. Baker, J.R. Ward, Chem. Rev. 92 (1991) 1729–1742.
[2] S. Talmage, A. Watson, V. Hauschild, et al., Curr. Org. Chem. 11 (2007) 285–298.
[3] A.J. Bobb, D.P. Arfsten, W.W. Jederberg, Mil. Med. 170 (2005) 52–56.
[4] C. Brevett, K.B. Sumpter, Main Group Chem. 9 (2010) 205–219.
[5] I.T. Ermakova, I.I. Starovoitov, E.B. Tikhonova, et al., Process Biochem. 38 (2002) 31–39.
[6] G.W. Wagner, P.W. Bartram, O. Koper, et al., J. Phys. Chem. B 103 (1999) 3225–3228.
[7] G.W. Wagner, O.B. Koper, E. Lucas, et al., J. Phys. Chem. B 104 (2000) 5118–5123.
[8] G.W. Wagner, Y.C. Yang, Ind. Eng. Chem. Res. 41 (2002) 1925–1928.
[9] B. Singh, T.H. Mahato, A.K. Srivastava, et al., J. Hazard. Mater. 190 (2011) 1053–1057.
[10] Y. Hou, H. An, Y. Zhang, et al., ACS Catal. 8 (2018) 6062–6069.
[11] G.W. Wagner, D.C. Sorrick, L.R. Procell, et al., Langmuir 23 (2007) 1178–1186.
[12] C. Changtong, D.W. Carney, L. Luo, et al., J. Photochem. Photobiol. A 260 (2013) 9–13.
[13] Y. Liu, S.Y. Moon, J.T. Hupp, et al., ACS Nano 9 (2015) 12358–12364.
[14] A.C. Serra, M. Pineiro, M.M. Pereira, et al., Chem. Phys. 280 (2002) 177–190.
[15] F. Nifiatis, J.C. Athas, K. Gunaratne, et al., Open Spectrosc. J. 5 (2011) 1–12.
[16] M. Ethirajan, Y. Chen, P. Joshi, et al., Chem. Soc. Rev. 40 (2010) 340–362.
[17] A.E. O'Connor, W.M. Gallagher, A.T. Byrne, Photochem. Photobiol. 85 (2010) 1053–1074.
[18] M. Zhao, S. Ou, C.D. Wu, Acc. Chem. Res. 47 (2014) 1199–1207.
[19] A. Fateeva, P.A. Chater, C.P. Ireland, et al., Angew. Chem. Int. Ed. 51 (2012) 7440–7444.
[20] C. Tanielian, C. Wolff, M. Esch, J. Phys. Chem. 100 (1996) 6555–6560.
[21] C. Tanielian, C. Schweitzer, R. Mechin, et al., Free Radical Biol. Med. 30 (2001) 208–212.
[22] Y. Liu, A.J. Howarth, J.T. Hupp, et al., Angew. Chem. Int. Ed. 54 (2015) 9001–9005.
[23] C.T. Buru, M.B. Majewski, A.J. Howarth, et al., ACS Appl. Mater. Interfaces 10 (2018) 23802–23806.
[24] C.L. Hill, Mol. Catal. 114 (1996) 1–3.
[25] J. Dong, J. Hu, Y. Chi, et al., Angew. Chem. Int. Ed. 56 (2017) 4473–4477.
[26] G.P. Yang, X.L. Zhang, Y.F. Liu, et al., Inorg. Chem. Front. 8 (2021) 4650–4656.
[27] G. Yang, X. Xie, M. Cheng, et al., Chin. Chem. Lett. 33 (2022) 1483–1487.
[28] G.P. Yang, K. Li, X.L. Lin, et al., Chin. J. Chem. 39 (2021) 3017–3022.
[29] M. Zhao, X.Y. Zhu, Y.Z. Li, et al., Tungsten 4 (2022) 121–129.
[30] T. Minato, D. Salley, N. Mizuno, et al., J. Am. Chem. Soc. 143 (2021) 12809–12816.
[31] C. Jahier, R. Touzani, S. El Kadiri, et al., Inorg. Chim. Acta 450 (2016) 81–86.
[32] J. Wang, C. Hu, M. Jian, et al., J. Catal. 240 (2006) 23–30.
[33] I.V. Kozhevnikov, Chem. Rev. 98 (1998) 171–198.
[34] C.T. Buru, M.C. Wasson, O.K. Farha, , ACS Appl Nano Mater 3 (2019) 658–664.
[35] Y. Li, Q. Gao, L. Zhang, et al., Dalton Trans. 47 (2018) 6394–6403.
[36] X.M. Guo, J. Mol. Struct. 892 (2008) 378–383.
[37] Z. Shi, Y. Zhou, L. Zhang, et al., RSC Adv. 4 (2014) 50277–50284.
[38] Z. Shi, Y. Zhou, L. Zhang, et al., Dalton Trans. 44 (2015) 4102–4107.
[39] T. Ishizuka, S. Ohkawa, H. Ochiai, et al., Green Chem. 20 (2018) 1975–1980.
[40] Y. Zhu, Y. Huang, Q. Li, et al., Inorg. Chem. 59 (2020) 2575–2583.
[41] C.J. Hallada, G.A. Tsigdinos, B.S. Hudson, J. Phys. Chem. 72 (1968) 4304–4307.
[42] M. Zhou, H. Guo, S.Q. Gao, et al., Chem. Res. Chin. Univ. 25 (2) (2009) 257–260.
[43] J.S. Lindsey, I.C. Schreiman, H.C. Hsu, et al., J. Org. Chem. 52 (1987) 827–836.
[44] S. Aronoff, J. Phys. Chem. 62 (1958) 428–431.
[45] S.Q. Liu, J.Q. Xu, H.R. Sun, et al., Inorg. Chim. Acta 306 (2000) 87–93.
[46] S.Q. Liu, J.Q. Xu, H.R. Sun, et al., Acta Phys. Chim. Sin. 17 (2001) 128–133.
[47] P.D. Bartlett, C.G. Swain, J. Am. Chem. Soc. 71 (1949) 1406–1415.
[48] R.I. Tilley, Aust. J. Chem. 46 (1993) 293–300.
[49] R.M. Narske, K.J. Klabunde, S. Fultz, Langmuir 18 (2002) 4819–4825.
[50] J. Jiang, R. Luo, X. Zhou, et al., Adv. Synth. Catal. 360 (2018) 4402–4411.
[51] H. Guo, H. Xia, X. Ma, et al., ACS Omega 5 (2020) 10586–10595.
[52] L.J. Chen, S. Chen, Y. Qin, et al., J. Am. Chem. Soc. 140 (2018) 5049–5052.
[53] G. Ayoub, M. Arhangelskis, X. Zhang, et al., Beilstein J. Nanotechnol. 10 (2019) 2422–2427.
[54] A.G. Mojarrad, S. Zakavi, Catal. Sci. Technol. 8 (2018) 768–781.